Rotational Mobility of the Fibrinogen Receptor Glycoprotein IIb/IIIa or Integrin $\alpha_{IIb}\beta_3$ in the Plasma Membrane of Human Platelets†

J. González-Rodríguez,*,‡ A. U. Acuña,‡ M. V. Alvarez,‡ and T. M. Jovin§

Unidad de Biofísica, Instituto de Química Física, CSIC, Serrano, 119, E-28006 Madrid, Spain, and Molecular Biology Department, Max Planck Institute for Biophysical Chemistry, D-37081 Göttingen, Germany

Received March 30, 1993; Revised Manuscript Received October 18, 1993®

ABSTRACT: Integrin $\alpha_{IIb}\beta_3$ or glycoprotein IIb/IIIa (GPIIb/IIIa, 228 kDa) is a Ca^{2+}-dependent, noncovalent heterodimer of glycoproteins IIb (GPIIb or α_{IIb}, 136 kDa) and IIIa (GPIIIa or β_3, 92 kDa), which serves as the receptor for fibrinogen and other adhesive proteins at the surface of activated platelets. We have determined the microsecond-range rotational motions of $\alpha_{IIb}\beta_3$ in resting platelets, in isolated plasma membranes, and reconstituted in 1-palmitoyl-2-oleoylphosphatidylcholine (POPC) bilayers. The measurements were based on the time-resolved phosphorescence anisotropy [$r(t)$] of erythrosin-labeled F(ab) fragments [Er-F(ab)] of monoclonal antibodies bound to $\alpha_{IIb}\beta_3$. In general, the $r(t)$ decays were satisfactorily fitted to the sum of the two exponential terms and a constant, from which the initial anisotropy ($r_{in} \approx$ 0.05–0.11), the short ($\phi_1 \approx$ 1–14 μs) and the long ($\phi_2 \approx$ 15–60 μs) rotational correlation times, and the limiting anisotropy ($r_\infty \approx$ 0.02–0.07) were obtained. The observed values depended on the platelet preparation, temperature, Ca^{2+} concentration, and the antibody used. In accordance with data on the order parameter and the viscosity of the lipid bilayer of the platelet plasma membrane, ϕ_2 and r_∞ of the $\alpha_{IIb}\beta_3$–Er-F(ab) complexes in the three preparations decreased with the increase of temperature, the $r(t)$ curves being fully reversible within the interval from 5 to 35 °C. On the basis of direct and indirect evidence, we exclude both $\alpha_{IIb}\beta_3$ size heterogeneity, due to autoassociation or heteroassociation with membrane or cytoskeletal proteins, and the heterogeneous distribution of $\alpha_{IIb}\beta_3$ between lipid environments differing in microviscosity as the source of the two correlation times. We interpret that ϕ_1 and ϕ_2 represent the segmental motion and global rotational relaxation of the $\alpha_{IIb}\beta_3$ monomer. The values of ϕ_2, estimated for the two transmembrane helices of the $\alpha_{IIb}\beta_3$ monomer, are much lower than the experimental values, which suggests that interactions between the lipid bilayer and ecto and/or endo domains of $\alpha_{IIb}\beta_3$ further limit the rotational mobility of $\alpha_{IIb}\beta_3$. Finally, prolonged calcium chelation at 35 °C, but not at 4 °C, immobilized the majority of $\alpha_{IIb}\beta_3$ in the membrane, in agreement with previous functional and biochemical studies in whole platelets and in isolated $\alpha_{IIb}\beta_3$ in solution.

The integrin $\alpha_{IIb}\beta_3$[1] or heterodimer GPIIb/IIIa is the major glycoprotein at the human platelet plasma membrane constituting 15% of the total membrane protein and 3% of the total platelet protein. It serves as the receptor for fibrinogen and other adhesive proteins, after platelet activation by a variety of agonists generated or exposed upon vascular lesion, and plays a primary role in platelet aggregation, platelet spreading on the exposed subendothelium, and clot retraction; i.e., in hemostasis (Plow & Ginsberg, 1989; Kieffer & Phillips, 1990; Hynes, 1992). $\alpha_{IIb}\beta_3$ (228 kDa) is a Ca^{2+}-dependent, noncovalent heterodimer formed by a disulfide-bonded two-chain subunit [GPIIb or α_{IIb} subunit (136 kDa): heavy chain α_{IIb}H (114 kDa) and light chain α_{IIb}L (22 kDa)] and a single-chain subunit (GPIIIa or β_3, 92 kDa) and, as predicted from the subunit's cDNA, has two transmembrane segments and two short cytoplasmic C-terminal tails (Kunicki et al., 1981; Heidenreich et al., 1990; Zimrin et al., 1990; Lanza et al., 1990; Rivas & González-Rodríguez, 1991; Rivas et al., 1991c; Calvete et al., 1992a,b). The only knowledge available so far on the molecular dynamics of $\alpha_{IIb}\beta_3$ had been derived from the observation by light and electron microscopy of the lateral movement and association induced either by addition of monoclonal antibodies and lectins or upon platelet activation (Loftus & Albrecht, 1984; Isenberg et al., 1987; White et al., 1990). Direct observation of the rotational dynamics of $\alpha_{IIb}\beta_3$ in the platelet membrane opens the possibility to probe the Ca^{2+}-, lipid-, and temperature-dependent stability of the heterodimer in the membrane (Rivas & González-Rodríguez,1991; Rivas et al., 1991a), the molecular mechanisms involved in the induction of receptor capacity (Hynes, 1992) and the auto- and heteroassociation upon platelet activation (Phillips et al., 1980; Loftus & Albrecht, 1984), and the modulation of the receptor mobility and function by the lipid composition of the bilayer of the plasma membrane (Mateo et al., 1991a).

In the 20 years since the first two reports on protein rotational mobility in biological membranes (Cone, 1972; Naqvi et al., 1973), a number of integral membrane proteins have been studied both in natural and in model membranes (Cherry, 1979; Thomas, 1986; Jovin & Vaz, 1989). In general, technical limitations and/or lack of detailed structural knowledge of the proteins of interest did not allow adequate consideration of side-chain and segmental motions in the nanosecond range.

† Supported by the DGICYT (Grants PM 88-022, PB 90-102, and PB 90-145) and by the Acción Integrada Hispano-Germana (1991–93, 65A).

* To whom correspondence should be addressed.

‡ CSIC.

§ Max Planck Institute for Biophysical Chemistry.

® Abstract published in *Advance ACS Abstracts,* December 1, 1993.

[1] Abbreviations: GPIIb/IIIa or $\alpha_{IIb}\beta_3$, heterodimer of glycoproteins IIb (or subunit α_{IIb}) and glycoprotein IIIa (or subunit β_3); GPIIbH (or α_{IIb}H) and GPIIbL (or α_{IIb}L), heavy (H) and light (L) chains of GPIIb; Er, erythrosin 5′-isothiocyanate; F(ab) and F(ab′)$_2$, F(ab) and F(ab′)$_2$ fragments, respectively, of enzymatic digestion of immunoglobulin G; mab, monoclonal antibody; POPC, 1-palmitoyl-2-oleoyl-phosphatidylcholine.

0006-2960/94/0433-266$04.50/0

However, the rotational motions in the microsecond and millisecond range dictated by the lipid bilayer have been studied extensively and interpreted in terms of molecular size, homogeneous or heterogeneous populations of rotational species (due to homo- or heteromolecular interactions), bilayer order and viscosity, and protein functional state. The challenge is to discriminate individual components in a complex anisotropy decay and assign the generally overlapping reorientational modes to specific molecular species or regimes.

In the present work, the rotational motions of $\alpha_{IIb}\beta_3$ in the microsecond range were investigated in resting platelets, in isolated plasma membrane fragments, and in $\alpha_{IIb}\beta_3$ reconstituted in 1-palmitoyl-2-oleoylphosphatidylcholine (POPC) bilayers, after binding erythrosin-labeled F(ab) fragments [Er·F(ab)] of monoclonal antibodies (mabs) whose epitopes have been already localized in the primary structure of α_{IIb} and β_3 (Calvete et al., 1991a,b). Analysis of the time-resolved phosphorescence anisotropy of $\alpha_{IIb}\beta_3$, measured by laser-kinetic spectroscopy, provided the first data on the restricted rotational mobility of $\alpha_{IIb}\beta_3$ in the platelet plasma membrane, which at 35 °C can be described by two rotational correlation times ($\phi_1 = 3 \pm 1$ μs and $\phi_2 = 29 \pm 2$ μs) and a residual anisotropy ($r_\infty = 0.023$). The dependence of these parameters on a number of experimental conditions was studied. We discuss the size-homogeneity of the $\alpha_{IIb}\beta_3$ rotating species and its homogeneous distribution in the lipid bilayer of the plasma membrane, and the relevance of the findings to the function of the fibrinogen receptor and by extension to the whole family of integrins.

MATERIALS AND METHODS

Materials. (*A*) *Reagents.* Erythrosin 5′-isothiocyanate (Er) was from Molecular Probes (Eugene, OR); pepsin and papain were from Worthington (Freehold, NJ), and glucose oxidase, catalase, and grade I apyrase were from Sigma. Chromatographic materials were from Pharmacia (Sweden). The other chemicals and biochemicals were of analytical or chromatographic grade.

(*B*) *Monoclonal Antibodies.* Murine mabs anti-α_{IIb} (M1, M3, M4, and M5) and anti-β_3 (P6, P37, and P97), all of the IgG class, were prepared according to immunization and fusion protocols and screening assays described previously (Melero & González-Rodríguez, 1984). Antibodies were purified from ascitic fluids after sequential 25%- and 50%-saturated $(NH_4)_2SO_4$ precipitation. The 50%-saturated $(NH_4)_2SO_4$ precipitates were subjected to affinity chromatography on protein A–Sepharose, according to the manufacturer's instructions. The purification process was monitored by SDS/PAGE and enzyme immunoassay, as described before (Calvete et al., 1991a,b).

F(ab) fragments of the purified antibodies were prepared by papain digestion at an antibody/enzyme (w/w) ratio of 100, at 37 °C for 4–12 h, depending on the particular antibody (Parham, 1986). The digestion products were subjected to ion-exchange chromatography on DEAE-Sephacel (Pharmacia). The F(ab) fragments eluted in the flow-through fraction, free of undigested IgG and the Fc fragments. Control of the digestion and F(ab) purification was by SDS/PAGE, enzyme immunoassay, and size-exclusion chromatography on Sephacryl S-100 or analytical ultracentrifugation (Beckman Model E).

$F(ab')_2$ fragments on the purified antibodies were prepared by pepsin digestion at an antibody/enzyme (w/w) ratio of 50, at 37 °C and pH 5 for 9–12 h, depending on the particular antibody (Johnstone & Thorpe, 1988). The digestion products were subjected first to ion-exchange chromatography on DEAE-Sephacel, and the flow-through fraction, which was free of undigested IgG and Fc fragments, was purified further by size-exclusion chromatography on Sephacryl S-200. Control of the digestion and of the purified $F(ab')_2$ was done by SDS/PAGE, enzyme immunoassay, and analytical ultracentrifugation.

(*C*) *Erythrosin Labeling of F(ab) Fragments.* Labeling of purified F(ab) fragments with Er was carried out at a dye/F(ab) molar ratio of 10, for 2 h at room temperature, at pH 8.0 and in the dark. The free dye was separated from Er-F(ab) by exclusion chromatography on a Sephadex G-25 column (1 cm × 30 cm), with a bed volume about 30 times larger than the sample volume. The labeling molar ratio [Er]/[F(ab)] was determined spectrophotometrically using $\epsilon_{540nm} = 85\ mM^{-1}\ cm^{-1}$ for Er and $\epsilon_{280nm} = 70\ mM^{-1}\ cm^{-1}$ for F(ab). The labeling molar ratio obtained for the different Er-F(ab)s ranged between 0.9 and 1.6. The Er-F(ab) solutions were stored at −130 °C, and the labeling ratio was checked before use, after clarification by ultracentrifugation in an Airfuge (Beckman).

Platelet Preparations. (*A*) *Whole Platelets.* Platelet concentrates were prepared immediately after blood extraction from healthy volunteer donors and left for 2 h at room temperature under gentle stirring with a rocking table. Washed platelets were prepared from platelet concentrates by three successive centrifugations at 120*g* for 4 min, to eliminate remaining erythrocytes and leukocytes. The supernatant was centrifuged at 1250*g* for 10 min and the pellet resuspended gently in washing buffer (35 mM citric acid, 103 mM NaCl, 5 mM KCl, 1 mM $CaCl_2$, 1 mM $MgCl_2$, and 5 mM glucose, pH 6.5) and washed twice in the same way. Finally, the platelets were resuspended in working buffer (137 mM NaCl, 2 mM KCl, 12 mM $NaHCO_3$, 0.3 mM $NaHPO_4$, 1 mM $CaCl_2$, 1 mM $MgCl_2$, 55 mM glucose, and 5 mM Hepes, pH 7.4) containing 25 μg/mL apyrase.

(*B*) *Platelet Plasma Membranes.* The platelet plasma membrane fraction was obtained from outdated platelet concentrates (72 h after blood collection in blood banks), after washing, glycerol loading, and subcellular fractionation by sucrose density gradient centrifugation, as described previously (Eirin et al., 1986).

(*C*) *Isolation of $\alpha_{IIb}\beta_3$.* The integrin $\alpha_{IIb}\beta_3$ was prepared from the platelet plasma membrane fraction as described elsewhere (Rivas et al., 1991b). Briefly, after differential extraction of platelet plasma membranes with Triton X-100, the 4% Triton supernatant was subjected to ion-exchange chromatography on a DEAE-Sephacel column equilibrated in 50 mM Tris-HCl (pH 7.0)/25 mM NaCl/1 mM $CaCl_2$ and 0.5% Triton X-100. The retained fraction, eluted with 0.5 M NaCl in the same buffer, contained 80–90% of the $\alpha_{IIb}\beta_3$ loaded onto the column, and was 4-fold-enriched in $\alpha_{IIb}\beta_3$ compared to the original membrane. This fraction was loaded onto a Sephacryl S-300 column equilibrated in 50 mM Tris-HCl (pH 7.4)/0.1 mM $CaCl_2$/0.025% NaN_3 and 0.2% Triton X-100. The second band eluted from this column was $\alpha_{IIb}\beta_3$ with no detectable phosphorus and constituted 85% of the $\alpha_{IIb}\beta_3$ originally loaded onto the column. The protein was concentrated on a DEAE-Sephacel column, rechromatographed on the same Sephacryl S-300 column, yielding 47 ± 8% of pure $\alpha_{IIb}\beta_3$ with respect to the $\alpha_{IIb}\beta_3$ content of the starting platelet membrane. All isolation steps were performed at 4 °C.

Incorporation of $\alpha_{IIb}\beta_3$ into Liposomes. We followed the same procedure used before (Rivas & González-Rodríguez,

1991). $\alpha_{IIb}\beta_3$ (2 mg/mL), in 50 mM Tris-HCl (pH 7.4)/0.1 mM $CaCl_2$/0.025% (w/v) NaN_3 and 2% (w/v) Triton X-100, was mixed with 1-palmitoyl-2-oleoylphosphatidylcholine (POPC) (Avanti Polar Lipids, Inc.) at a 1/3 (w/w) protein/lecithin ratio and left at room temperature for 1 h under gentle agitation. After centrifugation at 3000g for 10 min, the supernatant was diluted with the same buffer but without Triton, to bring the detergent concentration below its critical micellar concentration (0.016%) (Rivas & González-Rodríguez, 1991). The diluted mixture was concentrated in a membrane concentration device (Amicon) and subjected to several dilution–concentration cycles to eliminate the detergent. The $\alpha_{IIb}\beta_3$–lecithin bilayers formed in the final 2-mL sample were pelleted in conical tubes in a Beckman TL 100 ultracentrifuge at 60 000 rpm for 30 min. The $\alpha_{IIb}\beta_3$–lecithin pellet was resuspended at 1 mg/mL $\alpha_{IIb}\beta_3$ in working buffer containing 0.1 mM Ca^{2+} and 0.1 mM Mg^{2+}, and subjected to 4 cycles of 30 s of sonication under nitrogen and in an ice bath, using a microprobe at maximum power (Kontes-ultrasonicator).

$\alpha_{IIb}\beta_3$ Labeling with Er-F(ab) Fragments. Labeling of samples of 100 pmol of $\alpha_{IIb}\beta_3$ in whole platelets (6×10^8 platelets), in isolated platelet plasma membrane (155 μg of total membrane protein), and in POPC liposomes was performed in conical tubes using a 1–3-fold molar excess of Er-F(ab) fragments, at room temperature for 30–60 min and in the dark. Labeling in the presence of a 15-fold molar excess of unlabeled F(ab) with respect to the Er-F(ab) of the same antibody was routinely carried out as a control of unspecific labeling, which was found to be negligible in all cases. Samples were freed of unbound Er-F(ab) by sedimentation: platelets and platelet plasma membranes at 4000 rpm for 10 min and at 14 000 rpm for 15 min, respectively, in an Eppendorf centrifuge; and $\alpha_{IIb}\beta_3$–POPC liposomes at 60 000 rpm for 30 min in a Beckman TL 100 ultracentrifuge. The pellets were resuspended gently and washed twice in working buffer in the same way. Identical samples subjected to all the steps but incubated with unlabeled F(ab) or in working buffer alone were routinely prepared and used as controls of scatter and intrinsic phosphorescence in the phosphorescence anisotropy decay measurements.

Cross-Linking of $\alpha_{IIb}\beta_3$–Er-F(ab) Complexes in the Membrane with F(ab')$_2$ Fragments. $\alpha_{IIb}\beta_3$ in whole platelets, isolated platelet plasma membrane fragments, and POPC liposomes, labeled with Er-F(ab) of a given mab as described above, was incubated with F(ab')$_2$ of the same or other α_{IIb}- or β_3-specific mab at F(ab')$_2$/$\alpha_{IIb}\beta_3$ molar ratios between 1 and 3 for 30 min at room temperature in the dark. The samples were either washed once to free them of the excess of F(ab')$_2$ or transferred directly to the spectrometer. In some experiments, the order of incubation was altered, and whenever the pair of Er-F(ab) and F(ab')$_2$ fragments used came from the same antibody or from antibodies competing between themselves, then a very low signal, between 1/10 or 1/20 of the control sample [incubated only with Er-F(ab)], was obtained.

Calcium Chelation by EDTA at Different Temperatures. $\alpha_{IIb}\beta_3$ in whole platelets, isolated plasma membrane fragments, or POPC liposomes, labeled with Er-F(ab), was incubated in the spectrometer cuvette holder at the desired temperature, and upon recording the control phosphorescence anisotropy decay, EDTA in concentrated solution was added in the quantity required, according to the starting calcium concentration, pH, and temperature of the sample, to decrease the free calcium concentration to the desired value (Rivas & González-Rodríguez, 1991). The phosphorescence anisotropy decay was then obtained at different time intervals.

Time-Resolved Phosphorescence Anisotropy Measurements. Phosphorescence anisotropy measurements were carried out using a laser flash kinetic spectrometer and following a methodology that has been reviewed recently (Jovin & Vaz, 1989). Excitation of the erythrosin probe attached to the samples of interest was with a 10-ns, 1–4-mJ, 10-Hz vertically polarized pulse at 514 nm, generated by an excimer laser (EMG-50; Lambda Physics, Göttingen, FRG) pumping a dye laser (FL 2000, Lambda Physics) at 308 nm. The laser dye was Coumarin-307. The sample, about 50 nM $\alpha_{IIb}\beta_3$ (equivalent to 3×10^8 platelets/mL, 80 μg of total protein of platelet plasma membrane/mL, or 50 pmol/mL $\alpha_{IIb}\beta_3$ incorporated in POPC liposomes), was placed in a 5 mm × 5 mm quartz cuvette and freed of oxygen by addition of an enzyme mixture of glucose oxidase (25 μg/mL, final concentration) and catalase (15 μg/mL), and 50 mM glucose as the substrate. The erythrosin-polarized phosphorescence was measured through a train of optical filters: 2 mm of a saturated aqueous solution of potassium dichromate; a rotating film polarizer; a KV 550 filter (Schott, Mainz, FRG); and a RG 645 long-pass filter (Schott). The detector was an EMI 9816 QGA photomultiplier electronically gated to suppress the prompt fluorescence coincident with the excitation pulse (Yoshida et al., 1989). In general, records of 10^3 phosphorescence decays were accumulated for both emission polarized components (measured in alternation, 50 pulses of each component at a time). Files of these records were analyzed individually and as the sums of 3–5 files, so as to reduce the statistical noise component. The results of the latter analyses are reported in tables and figures. The decay curves of the total emission of phosphorescence, $S(t) = I_{\parallel}(t) + 2I_{\perp}(t)$, and phosphorescence anisotropy, $r(t) = [I_{\parallel}(t) - I_{\perp}(t)]/[I_{\parallel}(t) + 2I_{\perp}(t)]$, were generated from the parallel ($I_{\parallel}$) and the perpendicular ($I_{\perp}$) polarized components of the phosphorescence. The experimental $S(t)$ curves were fitted by a nonlinear least-squares method to multiexponential functions, with lifetimes τ_i, from where weighting factors were derived for the analyses of the $r(t)$ decays, which required the sum of two exponential terms and a constant, according to the expression

$$r(t) = \alpha_1 \exp(-t/\phi_1) + \alpha_2 \exp(-t/\phi_2) + r_\infty \qquad (1)$$

In eq 1, α_1 and α_2 are the preexponential terms (amplitudes) related to the contribution of each of the two exponential components; ϕ_1 and ϕ_2 are the rotational correlation times, related to the diffusion constants of the rotating species and therefore a measure of the rotational, segmental, and wobbling motions of the probe and the protein complex to which it is attached (Jovin & Vaz, 1989; Kinosita et al., 1984); and r_∞ is the limiting anisotropy, that is, the anisotropy of the equilibrium distribution of the probe after rotational depolarization, within the time range of the experiment. The initial anisotropy $r_{in.}$ was calculated as the sum of the decay amplitudes, α_1 and α_2, and r_∞.

RESULTS

$\alpha_{IIb}\beta_3$ Labeling with Er-F(ab) Fragments in Resting Platelets, Isolated Platelet Plasma Membranes, and POPC Bilayers. The α_{IIb}-specific (M_1, M_3, and M_5) and β_3-specific (P_6, P_{37}, and P_{97}) mabs have affinities for $\alpha_{IIb}\beta_3$ in the membrane and in solution in the 0.5–10 nM range (López, 1991). Thus, a 1–3-fold molar excess of Er-F(ab) over $\alpha_{IIb}\beta_3$ sufficed to saturate the $\alpha_{IIb}\beta_3$ samples. Unspecific labeling was checked by preincubation of the three $\alpha_{IIb}\beta_3$ preparations with a 15-fold molar excess of the Er-free F(ab) over the

Table 1: Representative Phosphorescence Lifetimes (τ_i) of Er-F(ab) Fragments of α_{IIb}- and β_3-Specific Monoclonal Antibodies Bound to Intact Human Platelets (P), Platelet Plasma Membrane Fragments (M), and $\alpha_{IIb}\beta_3$-Containing Liposomes (L)[a]

		P		M		L	
F(ab)	T (°C)	τ_1 (μs)	τ_2 (μs)	τ_1 (μs)	τ_2 (μs)	τ_1 (μs)	τ_2 (μs)
P97	5	13 (0.12)	156 (0.88)	13 (0.18)	155 (0.82)	12 (0.20)	147 (0.80)
	20	14 (0.13)	135 (0.87)	13 (0.18)	140 (0.82)	12 (0.22)	126 (0.78)
	35	15 (0.17)	111 (0.83)	12 (0.21)	110 (0.79)	11 (0.27)	106 (0.73)
P6	20	11 (0.4)	96 (0.6)	10 (0.4)	95 (0.6)	12 (0.19)	132 (0.81)
P37	20	14 (0.27)	105 (0.73)	14 (0.28)	110 (0.72)	12 (0.26)	105 (0.74)
M1	20	13 (0.27)	102 (0.73)	12 (0.26)	100 (0.74)	12 (0.25)	104 (0.75)

[a] The phosphorescence decays were obtained using 200-μs full scale in the digitizer. The numbers in parentheses are fractional amplitudes. Sample-to-sample variation in lifetimes and amplitudes was ~10%.

Er-F(ab) of the antibody used for labeling. The erythrosin phosphorescence intensity in these controls was less than 2% of that in Er-F(ab)-labeled samples, demonstrating that the nonspecific binding of Er-F(ab) to the three preparations was negligible.

Phosphorescence Intensity Decay Kinetics of Er-F(ab) Fragments in Solution and of the $\alpha_{IIb}\beta_3$–Er-F(ab) Complex in Membranes. The phosphorescence emission of the different Er-F(ab) bound to $\alpha_{IIb}\beta_3$ in the different membrane preparations was corrected for contributions from light scattering and intrinsic luminescence of the sample, by subtraction of the blank obtained with membrane samples treated in the same way as the labeled samples, except that Er-F(ab) was replaced by Er-free F(ab). The relative magnitude of the blank signals was negligibly small (0.01%). In general, the emission decays were satisfactorily fitted by two lifetimes (Table 1). Depending on the particular $\alpha_{IIb}\beta_3$ preparation, the labeling antibody used, and the observation time range, the short lifetime was 10–20 μs with a fractional amplitude of 0.12–0.40, whereas the long lifetime was in the 95–140-μs range and, as expected, decreased with increasing temperature. In general, there were little differences in the Er-F(ab) phosphorescence lifetimes, at a given temperature and observation time range, between samples of whole platelets, isolated plasma membranes, and liposomes; however, significant differences were observed for specific Er-F(ab) fragments such as P6, for which τ_2 and its amplitude were lower by 30 μs and 20%, respectively, in platelets and isolated membranes compared to liposomes (Table 1).

Phosphorescence Anisotropy Decay of Isolated Er-F(ab) Fragments in Viscous Solutions. The transient phosphorescence anisotropy of Er-F(ab) fragments of the mab P37 was measured at 68.8% (w/w) sucrose in water at 20 °C (η = 3.5 P) to assess the extent of emission depolarization caused by fast motions of the Er probe and by the segmental flexibility of the F(ab) fragment itself. The initial anisotropy, $r_{in.}$, was 0.08 ± 0.01, and the anisotropy decay was fitted to a monoexponential function (ϕ = 18 μs). These parameters are similar to those found before for F(ab) fragments from other mabs under the same experimental conditions (Pecht et al., 1991) and are in reasonable agreement with the rotational correlation time of 30 ns obtained for F(ab) fragments in water, using nanosecond fluorescence anisotropy (Oit et al., 1984).

Phosphorescence Anisotropy Decay of $\alpha_{IIb}\beta_3$–Er-F(ab) Complexes in Resting Platelets. The parameters of the time-resolved anisotropy decays of different Er-F(ab) fragments bound to resting platelets at several temperatures are included in Table 2, and typical decay curves are shown in Figure 1. The general pattern observed is a positive initial anisotropy ($r_{in.}$), a two-exponential decay, and a residual anisotropy (r_∞). The Er-F(ab)-P97 fragments were the most extensively used,

Table 2: Phosphorescence Anisotropy Decay Parameters of Er-F(ab) Fragments of α_{IIb}- and β_3-Specific Monoclonal Antibodies Bound to $\alpha_{IIb}\beta_3$ in Whole Platelets (P), Isolated Platelet Plasma Membrane Fragments (M), and POPC Liposomes (L)[a]

Er-F(ab)		T (°C)	α_1	ϕ_1 (μs)	α_2	ϕ_2 (μs)	$r_{in.}$	r_∞
P6	P	20	0.037	2 ± 1	0.022	29 ± 2	0.097	0.038
	M	20	0.040	1 ± 2	0.020	30 ± 5	0.099	0.039
	L	20	0.022	6 ± 1	0.020	39 ± 2	0.074	0.032
P37	P	20	0.017	6 ± 2	0.013	37 ± 3	0.072	0.042
	L	20	0.040	2 ± 1	0.014	15 ± 5	0.100	0.046
P97	P	5	0.016	9 ± 1	0.024	58 ± 2	0.087	0.047
		20	0.017	6 ± 2	0.020	48 ± 2	0.069	0.032
		35	0.032	3 ± 1	0.018	29 ± 2	0.073	0.023
	M	5	0.015	6 ± 1	0.021	60 ± 2	0.077	0.041
		20	0.021	6 ± 1	0.020	42 ± 2	0.070	0.030
		35	0.023	4 ± 2	0.017	27 ± 4	0.062	0.022
	L	5	0.016	8 ± 2	0.022	61 ± 3	0.077	0.032
		20	0.018	4 ± 2	0.021	35 ± 2	0.066	0.027
		35	0.033	3 ± 1	0.018	26 ± 2	0.073	0.022
M1	P	20	0.025	3 ± 2	0.010	23 ± 2	0.072	0.037
	M	20	0.01	8 ± 2			0.068	0.058
	L	20	0.010	4 ± 2	0.011	18 ± 2	0.069	0.048
M3	P	20	0.025	4 ± 2	0.014	50 ± 5	0.073	0.034
M5	P	5	0.09	5 ± 3	0.012	40 ± 2	0.072	0.051

[a] Errors based on sample-to-sample variation.

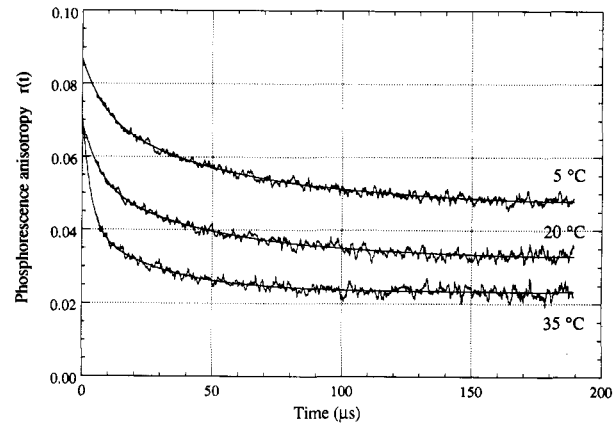

FIGURE 1: Phosphorescence anisotropy decay of Er-labeled F(ab) fragments of the β_3-specific mab P97 bound to intact platelets measured at the indicated temperatures, as described under Materials and Methods. The smooth lines are the decay curves generated with the best-fit parameters given in Table II.

and therefore we refer primarily to data obtained with this mab, unless stated otherwise. The apparent $r_{in.}$ values ranged from 0.05 to 0.10, indicating a >50% depolarization in the submicrosecond time range, since erythrosin r_0 = 0.26 (Jovin & Vaz, 1989). As expected, r_∞ and the rotational correlation times, ϕ_1 and ϕ_2, decreased with increasing temperature from 5 to 35 °C. ϕ_1 was in the 2–10-μs range, while ϕ_2 was around 60 μs at 5 °C and decreased to 25 μs at 35 °C, without large changes in their relative amplitude. r_∞ and the $r_\infty/r_{in.}$ ratio decreased with temperature, the actual average values for r_∞

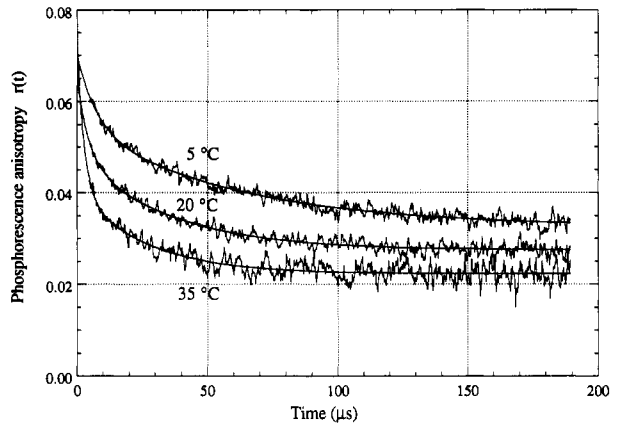

FIGURE 2: Time-resolved phosphorescence anisotropy of Er-F(ab) fragments of the mab P97 bound to $\alpha_{IIb}\beta_3$ reconstituted in POPC liposomes, as described under Materials and Methods, measured at the indicated temperatures. The smooth lines were generated with the best-fit parameters given in Table II.

being 0.047 at 5 °C, 0.032 at 20 °C, and 0.023 at 35 °C.

When the Er-F(ab)-labeled platelets were subjected to a temperature cycle starting at 20 °C, passing through 5 and 35 °C, and then returning to 20 °C, the anisotropy decay curves were fully reversible. The anisotropy decay parameters were not much influenced by the subunit specificity and the epitope location for the different F(ab) fragments used, compared with those of P97, except for the faster ϕ_2 found at 20 °C when using M1 (Table 2) and the single-exponential decay of anisotropy found at 20 and 35 °C when using M5 F(ab) fragments, with ϕ values in the 15–20-μs range (data not shown).

Phosphorescence Anisotropy Kinetics of $\alpha_{IIb}\beta_3$–Er-F(ab) Complexes in Isolated Platelet Plasma Membranes. To assess the contribution of heteroassociations of $\alpha_{IIb}\beta_3$ with non-membrane components, mainly skeletal proteins, to the rotational dynamics of $\alpha_{IIb}\beta_3$, a reduced number of experiments was carried out in isolated plasma membrane fragments labeled with Er-F(ab). It was found that the phosphorescence anisotropy decays and the temperature dependence of ϕ_1, ϕ_2, and r_∞ were quite similar to those in whole platelets (Table 2). One exception was provided by the Er-F(ab) fragments of M1, an antibody for the N-terminal region of the light chain of the α_{IIb} subunit. Both at 5 and at 20 °C, a single decay component was observed together with high values of r_∞ (0.06–0.07) and $r_\infty/r_{in.}$ (0.85) (Table 2).

Phosphorescence Anisotropy Kinetics of $\alpha_{IIb}\beta_3$–Er-F(ab) Complexes in POPC Bilayers. Two sets of experiments were performed after Er-F(ab) labeling of the isolated heterodimer reconstituted into POPC liposomes. The aim was to assess the contribution to the rotational dynamics of $\alpha_{IIb}\beta_3$ in whole platelets of both the heteroassociations of $\alpha_{IIb}\beta_3$ with other membrane components and the heterogeneous distribution of $\alpha_{IIb}\beta_3$ between different lipid environments. Comparison of the anisotropy decay parameter in liposomes with those in whole platelets and in isolated membrane fragments, using Er-F(ab)-P97, shows that ϕ_1 and ϕ_2 and their preexponential terms were quite similar in the three preparations, the major difference being in the r_∞ values at 5 °C, which were lower in the reconstituted heterodimer, as expected (Table 2 and Figure 2). The values of ϕ_2, observed at 20 °C and using the Er-F(ab) fragments of either P37 or M1, were shorter than those measured with either P6 or P97 at the same temperature. In addition, the $r_\infty/r_{in.}$ ratio observed with Er-F(ab)-M1 was higher than the ratio observed with other mabs, as also found above in isolated membrane fragments.

Table 3: Phosphorescence Anisotropy Decay Parameters of Er-F(ab) Fragments of α_{IIb}- and β_3-Specific Monoclonal Antibodies Bound to $\alpha_{IIb}\beta_3$ in Whole Platelets, Isolated Platelet Plasma Membranes, and POPC Bilayers[a]

Er-F(ab)	F(ab′)$_2$	α_1	ϕ_1 (μs)	α_2	ϕ_2 (μs)	$r_{in.}$	r_∞
		Whole Resting Platelets					
P37		0.020	3 ± 1	0.014	34 ± 3	0.071	0.037
	M5	0.020	6 ± 2	0.015	70 ± 10	0.072	0.037
P97		0.017	6 ± 2	0.020	48 ± 2	0.069	0.032
	M3	0.013	10 ± 2	0.021	56 ± 3	0.067	0.033
	M4	0.020	3 ± 1	0.014	54 ± 3	0.078	0.044
	M4	0.010	2 ± 1	0.026	43 ± 3	0.080	0.044
	M5	0.030	8 ± 3	0.013	60 ± 5	0.083	0.040
	M5	0.018	6 ± 2	0.023	47 ± 2	0.080	0.041
	P37	0.048	2 ± 1	0.024	37 ± 2	0.112	0.040
M5		0.020	20 ± 1			0.063	0.043
	P37	0.013	17 ± 2	0.007	61 ± 4	0.064	0.044
		Isolated Platelet Plasma Membrane Fragments					
P97		0.021	6 ± 1	0.020	42 ± 2	0.070	0.030
	M3	0.018	6 ± 2	0.018	43 ± 2	0.071	0.035
	M5	0.013	5 ± 2	0.020	43 ± 3	0.065	0.032
		POPC Bilayers					
P97		0.018	4 ± 2	0.021	35 ± 2	0.066	0.027
	M3	0.027	3 ± 1	0.024	36 ± 2	0.080	0.021
	M4	0.014	2 ± 1	0.022	32 ± 2	0.067	0.031
	M5	0.017	7 ± 2	0.018	50 ± 2	0.072	0.037
	P37	0.095	3 ± 1	0.020	22 ± 2	0.110	0.045

[a] Measured at 20 °C after incubation with F(ab′)$_2$ fragments of α_{IIb}- and β_3-specific monoclonal antibodies. Errors based on sample-to-sample variation.

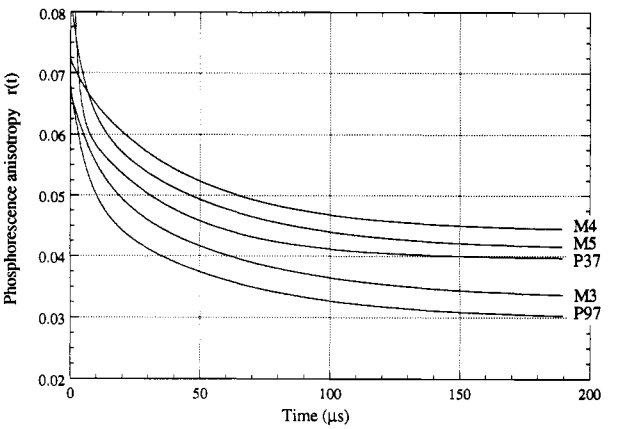

FIGURE 3: Phosphorescence anisotropy decay of Er-F(ab) fragments of the mab P97 bound to intact platelets measured at 20 °C, after incubation with F(ab′)$_2$ fragments of mabs P37, M3, M4, and M5, as described under Materials and Methods. The P97 curve is the control without incubation with any F(ab′)$_2$. For the sake of clarity, the original decay curves are omitted, and only the decay curves generated with the best-fit parameters are represented.

Cross-Linking of $\alpha_{IIb}\beta_3$–Er-F(ab) Complexes in Membranes by F(ab′)$_2$ Fragments. One way to assess the state of autoassociation of a molecular component within a supramolecular assembly is by specific homo-cross-linking. Thus, the $\alpha_{IIb}\beta_3$–Er-F(ab) complexes in the different preparations (whole platelets, isolated plasma membrane fragments, and POPC liposomes) were incubated with heterologous F(ab′)$_2$ fragments of α_{IIb}- and β_3-specific mabs, to observe the modifications in the phosphorescence anisotropy decay produced by $\alpha_{IIb}\beta_3$ cross-linking. As seen in Table 3 and Figure 3, most of the F(ab′)$_2$ fragments increased r_∞ in all the preparations and affected ϕ_2 to a variable extent. With two Er-F(ab)–F(ab′)$_2$ pairs (P37–M5 and M5–P37), ϕ_2 either doubled with respect to the control value (P37) or became detectable compared with the control for M5. In no case was an immobilization of $\alpha_{IIb}\beta_3$ by cross-linking observed.

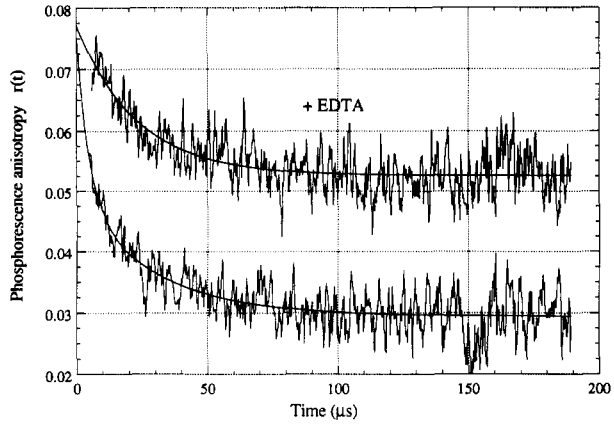

FIGURE 4: Phosphorescence anisotropy decay of Er-F(ab) fragments on the mab P97 bound to intact platelets measured at 35 °C, before and after incubation with EDTA at 35 °C for 50 min to lower the Ca^{2+} concentration to 0.1 nM, as described under Materials and Methods. The smooth lines were generated with the best-fit parameters.

Effect of Calcium Chelation on $\alpha_{IIb}\beta_3$–Er-F(ab) Complexes in the Membrane. Given the Ca^{2+}-dependent stability of the $\alpha_{IIb}\beta_3$ heterodimer, we studied the effect of free calcium concentration on the phosphorescence anisotropy decay of $\alpha_{IIb}\beta_3$–Er·F(ab) complexes in whole platelets and in isolated platelet plasma membrane fragments. We measured $r(t)$ at several temperatures, after decreasing the free calcium concentration at the required level by addition of EDTA (see Materials and Methods). After 50 min at 35 °C and 0.1 nM Ca^{2+}, the phosphorescence anisotropy decay of $\alpha_{IIb}\beta_3$–Er-F(ab) complexes in whole platelets was fitted to a single exponential ($\phi \approx 20$ μs) (Figure 4). The main modification observed was a substantial increase of the residual anisotropy from 0.030, at the physiological free calcium concentration, up to 0.053. In membrane fragments at 20 °C, calcium chelation with EDTA caused only a slight increase in r_∞.

DISCUSSION

We have shown in this study that a 50 nM concentration of $\alpha_{IIb}\beta_3$—either in whole platelets (3×10^8 platelets/mL, at about 8×10^4 copies of $\alpha_{IIb}\beta_3$ on the surface of a human platelet), or in platelet plasma membrane fragments (80 μg of total membrane protein/mL), or reconstituted in POPC liposomes (at a 1/600 $\alpha_{IIb}\beta_3$/POPC molar ratio)—is sufficient to perform transient phosphorescence anisotropy experiments and assess the rotational mobility of the fibrinogen receptor in the membrane, after specific and uniform labeling with Er-F(ab) fragments prepared from α_{IIb}- and β_3-subunit specific mabs directed to known epitopes in $\alpha_{IIb}\beta_3$ (Figure 5). Whole antibodies were avoided for labeling because they may bind to the Fc receptors present at the platelet surface or, being bivalent, may cross-link the $\alpha_{IIb}\beta_3$. It should be noted, however, that F(ab) fragments are not exempt from phenomena such as patching and capping and/or receptor–antibody internalization by endocytosis or by simple lateral diffusion to the surface-connected canalicular system of the platelet (Wencel-Drake, 1990).

A number of previous studies, dealing with the structure and motions of $\alpha_{IIb}\beta_3$, should be summarized before discussing the rotational motion of $\alpha_{IIb}\beta_3$ in the platelet plasma membrane. On the one hand, most of the 228 kDa of the heterodimer mass is extracellular, and of the three constitutive polypeptide chains, only two (α_{IIb}L and β_3) transverse the membrane and do so only once (Heidenreich et al., 1991; Zimrin et al., 1991; Lanza et al., 1991). Thus, the heterodimer has 2 short cytoplasmic tails (20–50 residues each) and 2 transmembrane segments, most probably in an α-helical conformation, which leads us to an estimate of the transmembrane cross-sectional area of 1.3 nm^2. The external domains have been mapped by epitope and ligand binding site location, proteolytic cleavage, and functional determinations [see Calvete et al. (1991a,b, 1992a,b) and references cited therein] from where indirect evidence on subunit and heterodimer molecular flexibility has been gathered. In addition, the molecular flexibility of $\alpha_{IIb}\beta_3$ is manifested by the head-two-tail forms seen in the electron micrographs (Keifer & Phillips, 1990; Rivas et al., 1991c) and by the rotational correlation times ($\phi_1 = 3 \pm 1$ ns, $\phi_2 = 15 \pm 3$ ns, and $\phi_3 = 150 \pm 20$ ns) determined in Triton X-100 solutions by time-resolved fluorescence anisotropy (M. P. Lillo, G. Rivas, J. González-Rodríguez, and A. U. Acuña, unpublished results). The longest correlation time, ϕ_3, is much shorter than expected for the overall rotation of any model compatible with the physical parameters for the $\alpha_{IIb}\beta_3$ monomer in solution (Rivas et al., 1991c). The rotational correlation times ($\phi_1 = 11 \pm 2$ μs, $\phi_2 = 65 \pm 4$ μs, and $r_\infty = 0.010$) have also been determined for isolated $\alpha_{IIb}\beta_3$ monomers directly labeled with eosin-ITC and reconstituted in egg yolk lecithin vesicles and measured by polarized laser-kinetic spectroscopy (A. U. Acuña, K. R. Naqvi, and J. González-Rodríguez, unpublished experiments). Finally, the lateral heterogeneity, order parameter, and microviscosity of the platelet plasma membrane (Mateo et al., 1991a,b) and POPC bilayers (Engel & Prendergast, 1981; Kinosita et al., 1984) have been determined by time-resolved fluorescence polarization.

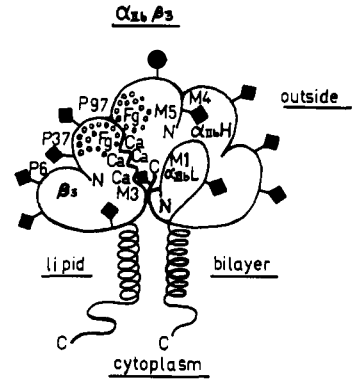

FIGURE 5: Pictorial scheme of $\alpha_{IIb}\beta_3$ in the human platelet membrane to indicate, to the best of our knowledge, the relative location of the epitopes of the mabs [M1 (α_{IIb}L 4–24), M3 (α_{IIb}H 849–856), M4 (α_{IIb}H 143–151), M5 (α_{IIb}H 550–558), P6 (β_3 300→), P37 (β_3 101–109), and P97 (β_3 260–300)] used in this work, the oligosaccharide chains (—♦), the calcium and fibrinogen binding sites, the transmembrane and cytoplasmic segments, and the N- and C-terminals of α_{IIb}H, α_{IIb}L, and β_3.

From the combined data above, we predict that a combination of several motions contributes to the observed phosphorescence anisotropy decay of $\alpha_{IIb}\beta_3$–Er-F(ab) in the three preparations studied here: the tethered motions (twisting, rocking, and bending) of the erythrosin probe itself and of the Er-F(ab) fragments bound to $\alpha_{IIb}\beta_3$; the segmental motions of small and large domains of $\alpha_{IIb}\beta_3$ to which the Er-F(ab) fragments are bound; and, finally, a combination of uniaxial rotation, about the membrane normal, and wobbling, about axes in the plane of the membrane, of the whole $\alpha_{IIb}\beta_3$ monomer or any of its putative homo- or heteroassociation products in the membrane.

Before a model for the rotational dynamics of $\alpha_{IIb}\beta_3$ in the membrane is discussed, some specific conclusions can be

derived from the phosphorescence anisotropy decays of the $\alpha_{IIb}\beta_3$–Er-F(ab) complexes. Thus, the $r_{in.}$ values found were always <50% of the r_0 values (~0.26) determined for the probe in rigid matrices (Jovin & Vaz, 1989), indicating a large submicrosecond depolarization, mainly due to motions of the probe and its macromolecular carrier, including the binding site on $\alpha_{IIb}\beta_3$. The r_∞ values and the $r_\infty/r_{in.}$ ratios, a measure of the angular restrictions imposed by the membrane, were in general found more dependent on the temperature than on the nature of the membrane preparation or the epitope location of the reporter antibody. On the other hand, a comparison of the rotational dynamic behavior of $\alpha_{IIb}\beta_3$ observed through a given Er-F(ab) (i.e., epitope) in whole platelets, in membrane fragments, and in POPC vesicles at 35 °C reveals no significant differences (Table 2). From this, we deduced that $\alpha_{IIb}\beta_3$, both in platelets and in isolated plasma membrane fragments, is not subjected to rotational constraints other than those taking place in POPC vesicles. This eliminates extrabilayer factors, such as platelet cytoskeleton and membrane skeleton, as well as interactions with heterologous membrane proteins. Furthermore, if we consider that $\alpha_{IIb}\beta_3$ in Triton X-100 solutions has no tendency to autoaggregate (Rivas et al., 1991c) and given the low $\alpha_{IIb}\beta_3$/POPC molar ratio (1/600) used in the reconstitution experiments reported here, one would not expect $\alpha_{IIb}\beta_3$ to aggregate in POPC vesicles. This is corroborated by the lack of abrupt changes in ϕ_1, ϕ_2, and r_∞ of $\alpha_{IIb}\beta_3$–Er-F(ab) in POPC vesicles over the 5–35 °C range. Therefore, it is reasonable to conclude that the $\alpha_{IIb}\beta_3$ monomer is the main species of the fibrinogen receptor present in whole platelets, isolated plasma membrane fragments, and POPC liposomes at physiological temperature.

It is significant that, although ϕ_1 and ϕ_2 of $\alpha_{IIb}\beta_3$ in platelets, membrane fragments, and POPC vesicles decrease to the same extent on decrasing temperature (Table 2), r_∞ in whole platelets and membrane fragments differs significantly from r_∞ in POPC vesicles already at 20 °C, and more pronouncedly at 5 °C. Our explanation for this is based on the lateral heterogeneity of the human platelet plasma membrane lipids (Mateo et al., 1991b). Thus, at 20 °C about 20% of the lipids are in solidlike (most probably cholesterol-rich) domains, the proportion of which should increase significantly at 5 °C (not measured). In contrast, POPC remains in a homogeneous liquid-crystalline phase at the same temperatures. Therefore, one would expect $\alpha_{IIb}\beta_3$ to be homogeneously distributed in POPC vesicles down to 5 °C. On the other hand, upon lowering the temperature below 35 °C, the platelet plasma membrane lipids gradually form solidlike domains, forcing $\alpha_{IIb}\beta_3$ to partition between the fluid phase and the solid domains. This would give rise to a population of $\alpha_{IIb}\beta_3$ molecules rotationally frozen in the microsecond time range, accounting for the higher r_∞ in the platelet plasma membrane compared with POPC vesicles. Alternatively, $\alpha_{IIb}\beta_3$ may aggregate within the liquid-crystalline phase with the same dynamic consequences. In both cases, the rotational correlation times of $\alpha_{IIb}\beta_3$ monomers remaining in the liquid-crystalline phase of the platelet membrane would be the same as those in POPC liposomes at the same temperature, as it is experimentally observed.

Before attempting an interpretation of the $r(t)$ decays of $\alpha_{IIb}\beta_3$ in the membrane and given the multiexponential character of the decays of both phosphorescence and phosphorescence anisotropy observed in the systems studied here, it is important to eliminate the possibility that any of the $r(t)$ time constants could be uncorrelated with the angular motions of the emitters. On the one hand, we have observed preparations in which the relative contribution of the fast emission component is only arround 10%, and yet the two anisotropy decay times are clearly resolved (Tables 1 and 2). On the other hand, there are preparations, such as membrane fragments labeled with M1 and the isolated F(ab) fragments in viscous sucrose solutions, where a single rotational correlation time together with two emission components was observed. Hence, we can exclude that the values of ϕ_1 and ϕ_2 are dependent on the phosphorescence lifetimes and, therefore, conclude that they are due to mechanical reorientational motions of $\alpha_{IIb}\beta_3$.

We turn now to the analysis of the phosphorescence anisotropy decays of $\alpha_{IIb}\beta_3$–Er-F(ab) complexes in the membrane based on two alternative models. If we assume that $\alpha_{IIb}\beta_3$ rotates as a rigid-cylinder around the membrane normal with diffusion coefficient $D_\parallel$—the ideal uniaxial rotational model—then the rate of rotation is given by the Saffman and Delbruck expression $D_\parallel = kT/4Ah\eta$, where A is the cross-sectional area of the transmembrane domain of $\alpha_{IIb}\beta_3$ ($2 \times 3.14 \times 0.45^2$ nm^2), h is the membrane thickness, and η is the membrane viscosity (Jovin & Vaz, 1 989). This model predicts for $\alpha_{IIb}\beta_3$ two rotational correlation times of relative magnitude $\phi_2/\phi_1 \approx 4$ and an average rotational correlation time somewhere between 150 ns for $\alpha_{IIb}\beta_3$ in pure POPC bilayers ($\eta_{20} \approx 0.5$ P) and 300 ns for $\alpha_{IIb}\beta_3$ in the platelet plasma membrane ($\eta_{20} \approx 1$ P). Even if a viscosity as high as 4 P is considered, the ϕ value predicted is not much higher than 1 μs. Given that the predicted rate of rotation of $\alpha_{IIb}\beta_3$ in the membrane is practically the same as that observed in solution, which is unacceptable, we conclude that this model is too unrealistic for the case studied here.

In the alternative model, the rate of wobbling motion, D_w, is given by the expression $D_w = kT/6\eta_c V_e f$, where V_e and f are the effective volume and the shape factor of the transmembrane domain, respectively, and η_c is the apparent viscosity in the wobbling cone (Kinosita et al., 1984). Here again, the predicted average rotational correlation time for $\alpha_{IIb}\beta_3$ wobbling is much smaller than the actual ϕ_2 value obtained, as was found before for other membrane proteins (Myers et al., 1992). Therefore, according to the evidence discussed above which indicates that the most likely rotating species at physiological temperature is the monomeric receptor, we conclude that none of the models based on rigid molecular structures predict the actual experimental data. To explain the observed dynamic behavior, it is necessary that some ecto or endo domains of $\alpha_{IIb}\beta_3$ may introduce other drag factors, besides membrane viscosity, which further slow down the $\alpha_{IIb}\beta_3$ rotational motions in the membrane.

Recent lateral diffusion measurements of chimeric membrane proteins [transmembrane proteins that were converted to glycosylphosphatidylinositol (GPI)-linked proteins or GPI-linked proteins that were converted to transmembrane-spanning proteins] have shown that the major determinant of the high mobility of GPI-linked proteins resides in the extracellular domain. In such cases, the lack of interaction of the extracellular domain of GPI-linked proteins with other membrane components allows a diffusion constrained only by the motion of the membrane anchor. In contrast, the membrane interactions of the ecto domain of membrane-spanning proteins reduce 10-fold their lateral diffusion coefficients, with respect to GPI-linked proteins (Zahng et al., 1992). Since the $\alpha_{IIb}\beta_3$ monomer is the only molecular species in POPC liposomes, then the main molecular interactions restricting $\alpha_{IIb}\beta_3$ rotational mobility should be those between POPC and ecto and/or endo domains of $\alpha_{IIb}\beta_3$. The retarding effect of the Er-F(ab) should be negligible, given

the similar results obtained with $\alpha_{IIb}\beta_3$–eosin (directly labeled with eosin-ITC) and $\alpha_{IIb}\beta_3$–Er-F(ab) incorporated in egg yolk lecithin and POPC liposomes, respectively (see above). The drag, which may involve electrostatic and hydrogen bond interactions after water exclusion between $\alpha_{IIb}\beta_3$ and the surface of the bilayer and/or protein acyl group penetration into the bilayer, must be of the same nature and occurs to the same extent in whole platelets, isolated membranes, and reconstituted liposomes. Membrane lipid composition would then modulate $\alpha_{IIb}\beta_3$ rotational dynamics not only via membrane viscosity but also through lipid head-group composition and protein acylation (Conforti et al., 1990; Smyth et al., 1992; Cierniewsky et al., 1992). It would be very interesting to know if the highly asymmetric lipid distribution in the platelet plasma membrane (Schroit & Zwaal, 1991), which is altered significantly after platelet activation, modulates $\alpha_{IIb}\beta_3$ rotational mobility.

If the above interpretation of the phosphorescence anisotropy decays of $\alpha_{IIb}\beta_3$ proves to be correct, then ϕ_1 must represent the substantial segmental motions of $\alpha_{IIb}\beta_3$ in the membrane. Although the accuracy of ϕ_1 is low, due to the instrumental limitations, its value decreases between a third and a half on going from 5 to 35 °C.

Two aspects remain to be discussed: the effect of $F(ab')_2$ fragments and calcium chelation on the rotational mobility of $\alpha_{IIb}\beta_3$. We have already concluded that $\alpha_{IIb}\beta_3$ is mainly in the monomer form in the membranes studied here. Therefore, it is expected that by being bivalent and monoclonal the $F(ab')_2$ fragments would (1) either not modify appreciably the $\alpha_{IIb}\beta_3$–Er-F(ab) phosphorescence anisotropy decays (2) or form $\alpha_{IIb}\beta_3$ dimers, but not oligomers, if the binding site in $\alpha_{IIb}\beta_3$ is suitably located so as to allow cross-linking of nearest neighbors. Thus, dimerization, the only cross-linking form observable, should be accompanied by an increase in ϕ_2 and in r_∞. Only two Er-F(ab)–$F(ab')_2$ pairs (P37–M5 and M5–P37) (Table 3) exhibited such behavior. With other pairs, either no change or at most a moderate increase in ϕ_2 and a consistent increase in r_∞ were observed. Unfortunately, we did not measure the extent of cross-linking by an alternative procedure. Thus, a full interpretation of these results requires the verification of cross-linking and determination of the fate of the F(ab')–$\alpha_{IIb}\beta_3$–Er-F(ab) complexes in whole platelets.

Calcium chelation at 35 °C, both in whole platelets and in isolated membrane fragments, caused an irreversible and substantial increase in r_{in} and r_∞ as well as important changes in the decay of the anisotropy, which could only be fitted to a single exponential with a rotational correlation time in the range of 20 μs. We regard these results as evidence for immobilization of the majority of the $\alpha_{IIb}\beta_3$ monomers, the residual decay being mainly due to the hindered segmental motions observed in the control samples. This interpretation fits with previous functional and biochemical studies in whole platelets (Zucker & Grant, 1978; Shattil et al., 1985; Pidard et al., 1986) and in isolated $\alpha_{IIb}\beta_3$ in solution (Rivas et al., 1991a,b), in which it was found that prolonged calcium chelation at physiological temperature produces a loss of platelet aggregability and autoassociation of the α_{IIb} and β_3 subunits.

CONCLUSIONS

The main conclusion of this work is that at physiological temperature, the large majority of $\alpha_{IIb}\beta_3$ in the plasma membrane of human platelets is in the monomer form, free from interactions with other membrane and cytoskeletal proteins. As expected, the $\alpha_{IIb}\beta_3$ rotational mobility in the microsecond range showed angular and rate constraints. Unexpectedly, however, the bilayer imposes a constraint on the rotational rate of $\alpha_{IIb}\beta_3$ much larger than that due to bilayer microviscosity. This effect is probably mediated through electrostatic and hydrogen bond interactions, after water is excluded in between $\alpha_{IIb}\beta_3$ and the bilayer surface, and/or penetration of $\alpha_{IIb}\beta_3$ acyl groups into the bilayer. This dynamic picture of $\alpha_{IIb}\beta_3$ is consistent with previous morphological, biochemical, and functional studies in which it was found that the fibrinogen receptor autoassociates and associates with cytoskeletal or membrane skeletal proteins only after platelet activation, receptor induction, and fibrinogen binding (Plow & Ginsberg, 1989; Kieffer & Phillips, 1990; Hynes, 1992). Furthermore, we know that the fibrinogen receptor is acylated (Cierniewsky et al., 1989) and its function is modulated by specific lipids (Smyth et al., 1992). On the other hand, the irreversible immobilization of $\alpha_{IIb}\beta_3$ observed after prolonged calcium chelation at physiological temperatures is consistent with the loss of platelet aggregability and α_{IIb}- and β_3-subunit autoassociation found before. Here we have also proposed that the fast rotational correlation time, ϕ_1, represents the slowest segmental motions of $\alpha_{IIb}\beta_3$ in the membrane. If that is confirmed by further work, then time-resolved phosphorescence anisotropy of $\alpha_{IIb}\beta_3$ in whole platelets and in model membranes would be an exceptionally good method to assess the mechanism of induction of the fibrinogen receptor ($\alpha_{IIb}\beta_3$*); fibrinogen binding to $\alpha_{IIb}\beta_3$*; autoassociation of $\alpha_{IIb}\beta_3$* in the platelet surface and the heteroassociation of $\alpha_{IIb}\beta_3$* with skeletal proteins; modulation of the structure, molecular dynamics, and function of $\alpha_{IIb}\beta_3$ and $\alpha_{IIb}\beta_3$* by lipid head groups, membrane viscosity, acylation, etc.; signal transduction inside-out and outside-in through $\alpha_{IIb}\beta_3$ and $\alpha_{IIb}\beta_3$*; and Ca^{2+}-, lipid-, and temperature-dependent stabilization of the $\alpha_{IIb}\beta_3$ heterodimer in the membrane.

Finally, since $\alpha_{IIb}\beta_3$ shares a structural and functional pattern with the rest of the members of the integrin family, the present conclusions may generally apply to the microsecond-range rotational dynamics of these molecules.

ACKNOWLEDGMENT

We thank Dr. R. K. Naqvi and Dr. W. L. C. Vaz for critical reading of the manuscript, Dr. M. M. López and Dr. G. A. Rivas for their help in the purification and modification of the monoclonal antibodies and GPIIb/IIIa, G. Pinillos and A. Vacas for technical assistance, R. Jenssen for secretarial assistance, T. Hernández for typing the manuscript, and the Blood Banks of the Hospitals Ramón y Cajal, La Paz, and Doce de Octubre (Madrid) and of the Universitätsklinikum (Göttingen) for providing us with outdated and fresh platelet concentrates.

REFERENCES

Calvete, J. J., Arias, J., Alvarez, M. V., López, M. M., Henschen, A., & González-Rodríguez, J. (1991a) *Biochem. J. 273*, 767–775.

Calvete, J. J., Arias, J., Alvarez, M. V., López, M. M., Henschen, A., & González-Rodríguez, J. (1991b) *Biochem. J. 274*, 457–463.

Calvete, J. J., Schäfer, W., Mann, K., Henschen, A., & González-Rodríguez, J. (1992a) *Eur. J. Biochem. 206*, 759–765.

Calvete, J. J., Mann, K., Alvarez, M. V., López, M. M., & González-Rodríguez, J. (1992b) *Biochem. J. 282*, 523–532.

Cierniewski, C. S., Krzeslowska, J., Pawlowska, Z., Witas, H., & Meyer, M. (1989) *J. Biol. Chem. 264*, 12158–12164.

Cone, R. A. (1972) *Nature (London), New Biol. 236*, 39–43.

Conforti, G., Zanetti, A., Pasquali-Ronchetti, I., Quaglino, D., Jr., Neyroz, P., & Dejana, E. (1990) *J. Biol. Chem. 265*, 4011–4019.
Cherry, R. J. (1979) *Biochim. Biophys. Acta 559*, 289–327.
Eirin, M. T., Calvete, J. J., & González-Rodríguez, J. (1986) *Biochem. J. 240*, 147–153.
Engel, L. W., & Prendergast, F. G. (1981) *Biochemistry 20*, 7338–7345.
Heidenreich, R., Eisman, R., Surrey, S., Delgrasso, K., Bennett, J. S., Schawartz, E., & Ponz, M. (1990) *Biochemistry 29*, 1232–1244.
Hynes, R. O. (1992) *Cell 69*, 11–25.
Isenberg, W. M., McEver, R. P., Phillips, D. R., Shuman, M. A., & Bainton, D. F. (1987) *J. Cell Biol., 104*, 1655–1663.
Johnstone, A., & Thorpe, R. (1988) *Immunochemistry in Practise*, pp 63–65, Blackwell, Oxford, U.K.
Jovin, T. M., & Vaz, W. L. C. (1989) *Methods Enzymol. 172*, 471–513.
Kieffer, N., & Phillips, D. R. (1990) *Annu. Rev. Cell Biol. 6*, 329–357.
Kinosita, K., Jr., Kawato, S., & Ikegami, A. (1984) *Adv. Biophys. 17*, 147–203.
Kunicki, T. J., Pidard, D., Rosa, J.-P., & Nurden, A. T. (1981) *Blood 58*, 268–278.
Lanza, F., Kieffer, N., Phillips, D. R., & Fitzgerald, L. A. (1990) *J. Biol. Chem. 265*, 18098–18103.
Loftus, J. C., & Albrecht, R. M. (1984) *J. Cell Biol. 99*, 822–829.
López, M. M. (1991) *Doctoral Thesis, Universidad de Valencia*, Valencia.
Mateo, C. R., Lillo, M. P., González-Rodríguez, J., & Acuña, A. U. (1991a) *Eur. Biophys. J. 20*, 41–52.
Mateo, C. R., Lillo, M. P., González-Rodríguez, J., & Acuña, A. U. (1991b) *Eur. Biophys. J. 20*, 53–59.
Melero, J. A., & González-Rodríguez, J. (1984) *Eur. J. Biochem. 141*, 421–427.
Myers, J. N., Holowka, D., & Baird, B. (1992) *Biochemistry 31*, 567–575.
Naqvi, R. K., González-Rodríguez, J., Cherry, R. J., & Chapman, D. (1973) *Nature (London), New Biol. 245*, 249–251.
Oi, V. T., Vuong, T. M., Hardy, R., Reidler, J., Dangl, J., Herzenberg, L. A., & Stryer, L. (1984) *Nature 307*, 136–140.
Parham, P. (1986) in *Handbook of Experimental Immunology* (Weir, D. M., Herzenberg, L. A., & Blackwell, C., Eds.) Vol. 1, Blackwell, Oxford, U.K.
Pecht, I., Ortega, E., & Jovin, T. M. (1991) *Biochemistry 30*, 3450–3458.
Pidard, D., Didry, D., Kunicki, T. J., & Nurden, A. T. (1986) *Blood 67*, 604–611.
Phillips, D. R., Jennings, L. K., & Edwards, H. H. (1980) *J. Cell Biol. 86*, 77–86.
Plow, E. F., & Ginsberg, M. H. (1989) *Prog. Hemostasis Thromb. 9*, 117–156.
Rivas, G. A., & González-Rodríguez, J. (1991) *Biochem. J. 276*, 35–40.
Rivas, G. A., Usobiaga, P., & González-Rodríguez, J. (1991a) *Eur. Biophys. J. 20*, 287–292.
Rivas, G. A., Calvete, J. J., & González-Rodríguez, J. (1991b) *Protein Expression Purif. 2*, 248–255.
Rivas, G. A., Aznárez, J. A., Usobiaga, P., Sáiz, J. L., & González-Rodríguez, J. (1991c) *Eur. Biophys. J. 19*, 335–345.
Schroit, A. J., & Zwaal, R. F. A. (1991) *Biochim. Biophys. Acta 1071*, 313–329.
Shattil, S. J., Brass, L. F., Bennett, J. S., & Pandhi, P. (1985) *Blood 66*, 92–98.
Smyth, S. S., Hillery, C. A., & Parise, L. V. (1992) *J. Biol. Chem. 267*, 15568–15577.
Thomas, D. D. (1986) in *Analysis of Membrane Proteins* (Regan, C. I., & Cherry, R. J., Eds.) pp 377–431, Chapman and Hall, London.
Wencel-Drake, J. D. (1990) *Am. J. Pathol. 136*, 61–70.
White, J. G., Leistikow, L., & Escolar, G. (1990) *Blood Cells 16*, 43–72.
Yoshida, T. M., Jovin, T. M., & Barisas, B. G. (1989) *Rev. Sci. Instrum. 60*, 2924–2928.
Zahng, F., Crise, B., Su, B., Hou, Y., Rose, J. K., Bothwell, A., & Jackson, K. (1992) *J. Cell Biol. 115*, 75–84.
Zimrin, A. B., Gidwitz, S., Lord, S., Schwartz, E., Bennett, J. S., White, G. C., II, & Poncz, M. (1990) *J. Biol. Chem. 265*, 8590–8595.
Zucker, M. A., & Grant, R. A. (1978) *Blood 52*, 505–514.